Dyes and Pigments 83 (2009) 291–296

Contents lists available at ScienceDirect

Dyes and Pigments

journal homepage: www.elsevier.com/locate/dyepig

The synthesis and properties of novel, functional azobenzene based metal complexes

Xulin Xia [a,*], Leong Huat Gan [b], Xiao Hu [c]

[a] School of Chemical Engineering, Anhui University of Technology, 59 Hudong Road, Maanshan, Anhui 243002, PR China
[b] Natural Science Academic Group, National Institute of Education, Nanyang Technological University, 1 Nanyang Walk, Singapore 637616, Singapore
[c] School of Material Engineering, Nanyang Technological University, 50 Nanyang Avenue, Singapore 639798, Singapore

ARTICLE INFO

Article history:
Received 14 February 2009
Received in revised form
7 May 2009
Accepted 7 May 2009
Available online 13 June 2009

Keywords:
Metal complex
Azobenzene
Photoisomerization
Photoresponsive
Photo-luminescence
Single crystal

ABSTRACT

Azobenzene-containing metal complexes with different carbon chain lengths connecting the azobenzene moiety and the diamine $ZnCl_2$ unit were characterized using spectrophotometric methods as well as thermal and X-ray diffractometric analysis. The length of the chain between the azobenzene moiety and the diamine metal complex influences both the thermal and fluorescent behaviour of the bi-functional compounds. Combining the azobenzene chromophore with the metal complex results in remarkably high azobenzene isomerization as well as two-band fluorescence emission centered at 290 and 560 nm respectively, imparted by the metal complex component. A holographic image inscription and readout experiment of one of the metal complexes in a poly(methyl methacrylate) matrix is described.

1. Introduction

Azobenzene containing compounds have been intensively studied for both theoretical and practical purposes for many years. They are widely commercially available and are used as dyes and, more recently, have been applied to photoresponsive molecular switches and materials. They have found broad application in nonlinear optics, optical storage media, chemosensors and optical switches [1–4]. For the purpose of realizing a desired photoresponsive functionality, the development of new designs, strategies, and the improvement of candidate materials have been undertaken enthusiastically in recent years.

Azo transitional metal complexes represent an interesting field of azobenzene chemistry [5,6], as they combine the optical, redox, and magnetic properties of the metal complex with the photoisomerization properties of the azo functional group. The azobenzene group as a ligand can form metal complexes with transitional metals, such as Pt and Pd [7,8], as a consequence of bonding between the azo group and the transition metal, azobenzene photoisomerization no longer occurs, a feature that limits the variety of azobenzene functionality.

Previously, azobenzene-based functional polymeric materials have been described [9,10] which show promising photoresponsive characteristics. This paper concerns further exploration of azobenzene functionality by connecting an azobenzene group to a Zn metal complex with the intention of combining the properties of the metal-complex with the extraordinary physical characteristics of an azobenzene chromophore which might lead to the generation of novel materials.

2. Experimental

2.1. General methods

Absolute ethanol, methanol, n-hexane, diethylether, acetone and chloroform were purchased from Aldrich and were stored over 4 Å molecular sieves. N,N-dimethyl formamide (DMF, Merck), tetrahydrofuran (THF, Fisher Scientific) were distilled under reduced nitrogen pressure from CaH_2 and subsequently stored over 4 Å molecular sieves. 4-Hydroxyazobenzene, 1,4-dibromobutane and 1,6-dibromohexane were purchased from Fluka and used as received.

^1H NMR spectra were recorded on a BRUKER 400 NMR spectrometer at 400 MHz in deuterated solvents with tetramethylsilane (TMS) as an internal standard. IR spectra were recorded on a Perkin–Elmer FT-IR spectrometer 1725X on KBr discs. UV spectra

---

* Corresponding author. Fax: +86 555 2311552.
E-mail address: xlxia@ahut.edu.cn (X. Xia).

0143-7208/$ – see front matter © 2009 Elsevier Ltd. All rights reserved.
doi:10.1016/j.dyepig.2009.05.015

were recorded in various solvent using a Hewlett Packard UV/VIS 8425A diode array spectrophotometer, fluorescent measurements were made on an SHIMADZU RF-5301 PC spectrofluorophotometer.

Thermal phase transitions were measured with a TA instrument 2920 Modulated DSC using a scan speed of 5 °C/min. Elemental analyses were performed using a Leco CHNS – 932 elemental analyzer. Crystallographic data were collected on a single crystal by Siemens P4 X-ray diffractometer with Mo Kα radiation by θ/2θ scan. The UV light for irradiation is generated by a 500 W mercury lamp cooled by a circulated cooling water system with a light filter centered at 360 nm and the light intensity is ca 2.0 mw/cm^2. Azobenzene photoisomerization experiments were carried out using a 1 cm quartz cuvette to measure absorbance changes immediately after the sample solution in cuvette had been subject to UV light or heat treatment.

2.2. Synthesis and characterization of azobenzene-containing metal complexes

The synthesis route for the metallomesogens **IIIa**, **b** is shown in Fig. 1.

*2.2.1. Synthesis of 4-(4-bromobutyloxy) azobenzene(**Ia**)*

To a 250 ml three-neck round bottomed flask, 7.05 mL (12.9 g, 60 mmol) 1,4-dibromobutane, 2.76 g (20 mmol) K_2CO_3, 0.12 g (0.7 mmol) KI and 30 ml acetone were added. To a 250 mL pressure equalising dropping funnel, 4.0 g (20 mmol) 4-hydroxyazobenzene (HAZ) in 40 mL acetone were added. The HAZ solution was added drop-wise to the flask. The reaction mixture was magnetically stirred and heated by an oil bath to a constant reflux temperature(ca. 60 °C) for about 13 h. The salts formed were filtered with a Buchner funnel, then washed with acetone. The solvent of the filtrate was evaporated off by a rotary evaporator. The crude product was washed with very small amount of ethanol and chloroform, then recrystallized from methanol twice and dried in vacuum oven at 40 °C. Yield: 3.264 g (48.5%).

m.p.: 86 °C. (DSC, 10 °C/min)

FT-IR (KBr, cm^{-1}): 2955 (aliphatic C–H stretch); 1606, 1504 (aromatic C=C ring stretch); 1413 (–N=N–); 1255 (C–O stretch); 1144 (C–N); 835 (aromatic C–H, 1,4-disubstituted benzene ring).

^{1}H NMR ($CDCl_3$, 400 MHz): δ_{ppm} = 1.81 (m, 2H, $-CH_2CH_2\underline{CH_2}CH_2Br$), 1.96 (m, 2H, $-CH_2\underline{CH_2}CH_2CH_2Br$), 3.78 (s, 2H, $-(CH_2)_3\underline{CH_2}Br$), 4.12 (s, 2H, $-\underline{CH_2}(CH_2)_3Br$), 7.03 (d, 2H, ArH), 7.52 (m, 3H, ArH), 7.93 (m, 4H, ArH).

Anal. Calcd for $C_{16}H_{17}N_2OBr$: C, 57.67%; H, 5.41%; N, 8.41%. Found: C, 57.24; H, 5.48%; N, 8.15%.

*2.2.2. Synthesis of 4-(6-bromohexyloxy)azobenzene (**Ib**)*

The synthesis of 4-(6-bromohexyloxy)azobenzene (**Ib**) was accomplished using an identical method to that used for 4-(4-bromobutyloxy)azobenzene (**Ia**). Yield: 53%. m.p.: 76.1 °C. (DSC, 10 °C/min)

FT-IR (KBr, cm^{-1}): 2941 (aliphatic C-H stretch); 1605, 1501 (aromatic C=C ring stretch); 1472 (–N=N–); 1258 (C–O stretch); 1143 (C–N); 842 (aromatic C–H, 1,4-disubstituted benzene ring).

^{1}H NMR ($CDCl_3$, 400 MHz): δ_{ppm} = 1.57 (m, 4H, $-CH_2CH_2\underline{(CH_2)_2}CH_2CH_2Br$), 1.85–1.96 (m, 4H, $-CH_2\underline{CH_2}(CH_2)_2\underline{CH_2}CH_2Br$), 3.46 (t, 2H, $-(CH_2)_5\underline{CH_2}Br$), 4.07 (t, 2H, $-O\underline{CH_2}(CH_2)_5Br$), 7.03 (d, 2H, ArH), 7.52 (m, 3H, ArH), 7.93 (m, 4H, ArH).

Anal. Calcd for $C_{18}H_{21}N_2OBr$: C, 59.84%; H, 5.86%; N, 7.75%. Found: C, 59.41; H, 5.69%; N, 7.62%.

*2.2.3. Synthesis of 4-(4-(N,N,N′-trimethylethylenediamino)butyloxy) azobenzene(**IIa**)*

To a 100 ml one-neck round bottomed flask connected to a condenser, 1.0 g (3 mmol) **Ia,** N,N,N′–trimethylethylenediamine 0.88 mL (6.9 mmol), NaOH 0.12 g (3 mmol), 0.42 mL (3 mmol) triethylamine and 25 mL acetone were added. The mixture was magnetically stirred and heated in a water bath to a constant reflux temperature(ca. 60 °C) for 5 h. The solvent was evaporated by rotary evaporator to near dryness. Ethyl acetate (15 mL) and benzene (15 mL) were added to extract the product. The organic solution was washed with distilled water (10 mL) 3 times. The organic layer was separated and dried with $MgSO_4$. The organic solution was separated from $MgSO_4$ by pasteur pipette. The solvent was evaporated to a constant weight using a vacuum oven. The pasty product of **IIa** was 0.460 g. Yield: 43.3%.

^{1}H NMR ($CDCl_3$, 400 MHz): δ_{ppm} = 1.60–1.80 (m, 4H, $-OCH_2\underline{CH_2CH_2}CH_2-$), 2.25 (s, 9H, $-CH_2(\underline{CH_3})NCH_2CH_2N(\underline{CH_3})_2$), 2.46 (m, 6H, $-\underline{CH_2}(CH_3)N\underline{CH_2CH_2}N(CH_3)_2$), 4.07 (t, 2H, $-O\underline{CH_2}(CH_2)_3N-$), 7.00 (d, 2H, ArH), 7.49 (m, 3H, ArH), 7.90 (m, 4H, ArH).

Anal. Calcd for $C_{21}H_{30}N_4O$: C, 71.15%; H, 8.53%; N, 15.80%. Found: C, 70.71; H, 8.67%; N, 15.43%.

*2.2.4. Synthesis of 4-(6-(N,N,N′-trimethylethylenediamino)hexyloxy) azobenzene (**IIb**)*

The synthesis of **IIb** was accomplished using an identical method to that used for **IIa** with 61% yield.

FT-IR (KBr, cm^{-1}): 2941 (aliphatic C–H stretch); 1602, 1499 (aromatic C=C ring stretch); 1475 (–N=N–); 1251 (C–O stretch); 1141 (C-N); 846 (aromatic C-H, 1,4-disubstituted benzene ring).

^{1}H NMR ($CDCl_3$, 400 MHz): δ_{ppm} = 1.52–1.75 (m, 8H, $-OCH_2\underline{(CH_2)_4}CH_2-$), 2.25 (s, 9H, $-CH_2(\underline{CH_3})NCH_2CH_2N(\underline{CH_3})_2$), 2.46 (m, 6H, $-\underline{CH_2}(CH_3)N\underline{CH_2CH_2}N(CH_3)_2$), 4.07 (t, 2H, $-O\underline{CH_2}(CH_2)_5N-$), 7.02 (d, 2H, ArH), 7.49 (m, 3H, ArH), 7.90 (m, 4H, ArH).

Anal. Calcd for $C_{23}H_{34}N_4O$: C, 72.21%; H, 8.96%; N, 14.65%. Found: C, 71.73; H, 8.61%; N, 14.38%.

*2.2.5. Synthesis of 4-(4-(N,N,N′–trimethylethylenediamino) butyloxy) azobenzene – zinc chloride complex (**IIIa**)*

To a 10 mL flask, 0.05 g **IIa** dissolved in ca. 1.0 mL acetone was added. In another 10 mL flask, 0.02 g freshly dried $ZnCl_2$ dissolved in ca. 1.0 mL acetone was added. While under magnetic stirring, the $ZnCl_2$ solution was added drop-wise to the solution of **IIa**. The mixture was then kept at 40 °C for half an hour in a water bath before the solvent was evaporated off. The solid obtained was recrystallized from methanol and then recrystallized from ethanol.

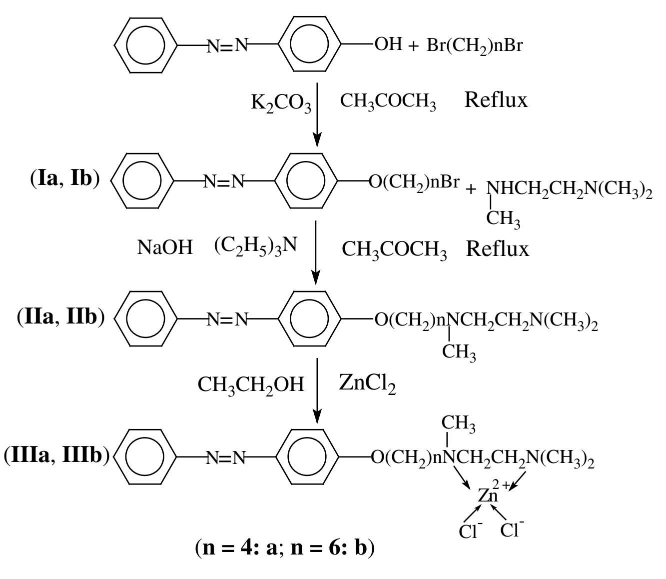

Fig. 1. The synthesis route for azobenzene-containing metal complexes.

It was then washed with cold ethanol, finally dried in a vacuum oven. Yield: 42%.

m.p.: 151.6 °C. (DSC, 10 °C/min)

FT-IR (KBr, cm^{-1}): 2948 (aliphatic C–H stretch); 1602, 1501 (aromatic C=C ring stretch); 1471 (–N=N–); 1254 (C–O stretch); 1143 (C–N); 839 (aromatic C–H, 1,4-disubstituted benzene ring).

^{1}H NMR (CDCl$_3$, 400 MHz): δ_{ppm} = 1.82–1.96 (m, 4H, $-OCH_2\underline{CH_2}\underline{CH_2}CH_2-$), 2.58–3.13 (m, 15H, $-\underline{CH_2}(\underline{CH_3})N\underline{CH_2}\underline{CH_2}N(\underline{CH_3})_2$), 4.10 (t, 2H, $-O\underline{CH_2}(CH_2)_3N-$), 7.02 (d, 2H, ArH), 7.49 (m, 3H, ArH), 7.90 (m, 4H, ArH).

Anal. Calcd for $C_{21}H_{30}N_4OZnCl_2$: C, 51.39%; H, 6.16%; N, 11.42%. Found: C, 51.30; H, 6.27%; N, 11.30%.

2.2.6. Synthesis of 4-(6-(N,N,N′-trimethylethylenediamino) hexyloxy) azobenzene – zinc chloride complex (*IIIb*)

The synthesis of **IIIb** was accomplished using an identical method to that used for **IIIa** with 40% yield.

m.p.: 158.4 °C. (DSC, 10 °C/min)

FT-IR (KBr, cm^{-1}): 2941 (aliphatic C–H stretch); 1603, 1504 (aromatic C=C ring stretch); 1471 (–N=N–); 1258 (C–O stretch); 1144 (C–N); 841 (aromatic C–H, 1,4-disubstituted benzene ring).

^{1}H NMR (CDCl$_3$, 400 MHz): δ_{ppm} = 1.40–1.96 (m, 8H, $-OCH_2(\underline{CH_2})_4CH_2-$), 2.52–3.10 (m, 15H, $-\underline{CH_2}(\underline{CH_3})N\underline{CH_2}\underline{CH_2}N(\underline{CH_3})_2$), 4.07 (t, 2H, $-O\underline{CH_2}(CH_2)_5N-$), 7.02 (d, 2H, ArH), 7.49 (m, 3H, ArH), 7.90 (m, 4H, ArH).

Anal. Calcd for $C_{23}H_{34}N_4OZnCl_2$: C, 53.24%; H, 6.61%; N, 10.80%. Found: C, 53.14; H, 6.70%; N, 10.65%.

3. Results and discussion

3.1. Synthesis

The reaction between 4-hydroxyazobenzene and either 1,4-dibromobutane or 1,6-dibromohexane was carried out using potassium carbonate and a catalytic amount of potassium iodide. The molar ratio had to be at least 3:1 of 1,4-dibromobutane (or 1,6-dibromohexane) to 4-hydroxyazobenzene to ensure that only one bromine atom was substituted.

The product (**Ia** or **Ib**) was reacted with N, N, N′-trimethylethelenediamine in an alkaline media with triethylamine to trap the produced hydrobromide. The reaction was completed within several hours, but the purification of the pasty product was difficult and included repeated extraction with organic solvents and washing with aqueous acid and water before drying in a vacuum oven at 40 °C for 48 h.

The metal complexes were readily obtained by treating the diamine ligands (**IIa** or **IIb**) with $ZnCl_2$ in acetone. The crystalline products were grown from ethanol for **IIIa** or ethanol and acetone mixed solvent (ethanol:acetone 1:5) for **IIIb**. Other transition metals, such as Cu^{2+}, Ni^{2+} and Co^{2+} were also used to prepare azobenzene containing metal complexes in the same manner as that of Zinc ion. However, none of these lead to the formation of a metal complex. This feature could be explained by assuming that the ligand trimethyl ethylene diamine, has a specific spacial configuration when connected with the azobenzene moiety which enables it to form complex with Zinc rather than other metal ions tested.

3.2. Thermal analysis

Examination of the DSC traces of compounds **IIIa** and **IIIb** (Fig. 2), revealed that **IIIb** exhibited one phase transition at about 158 °C from crystal phase to an isotropic melted phase. On the other hand, **IIIa** showed three phase transitions i.e. from crystal to a glassy state at temperature around 10 °C, then to a cold solid state phase transition [11] at about 79 °C, and finally to an isotropic state transition at 151.6 °C.

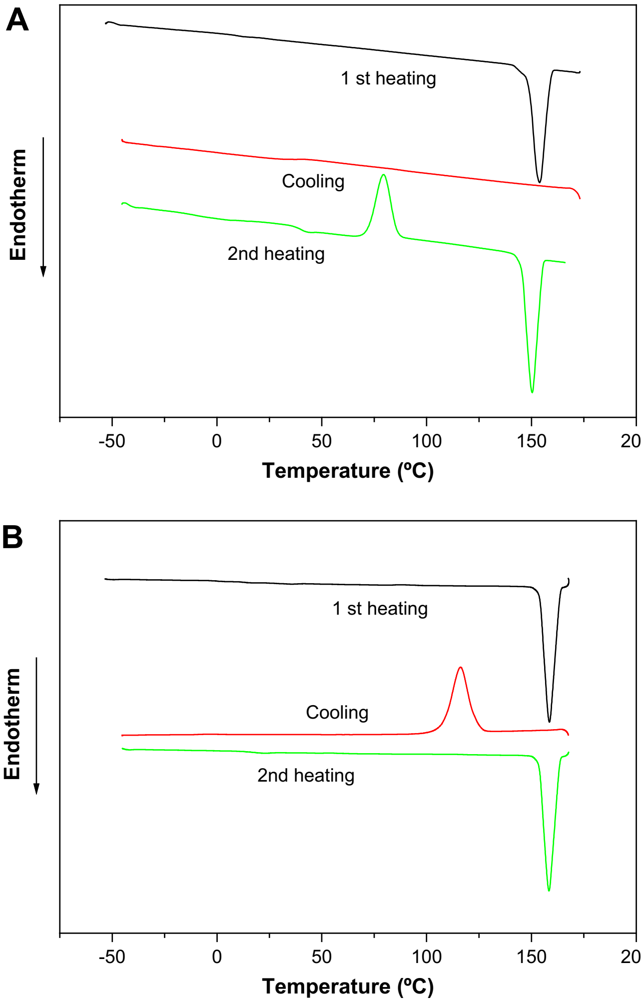

Fig. 2. The DSC traces of **IIIa** (**A**) and **IIIb** (**B**).

The marked thermal phase differences between these two seemly similar compounds indicate that the carbon chain length (4 and 6 in this instance) between the azobenzene moiety and the diamine zinc complex has a vital effect on whether different conglomerate states could be formed or not when heat treatment is conducted.

3.3. X-ray crystal diffraction analysis

The crystal of **IIIa** grown at room temperature was examined by X-ray diffraction. The crystal structure and matrix arrangement are shown in Fig. 3 and Fig. 4 respectively. The crystal data and refinement for **IIIa** is listed in Table 1. From the crystal structure and matrix arrangement it was found that **IIIa** molecules are arranged in a head-to-head and tail-to-tail way, so that the static electronic

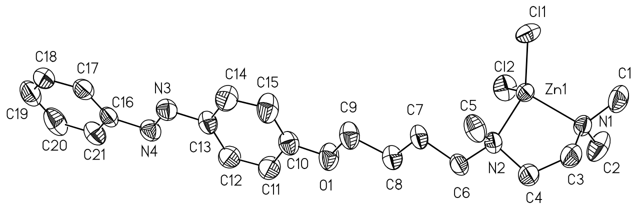

Fig. 3. Molecular structure of the complex **IIIa** by X-ray crystal measurement. An ORTEP drawing showing the atomic labeling scheme (H atoms omitted for clarity).

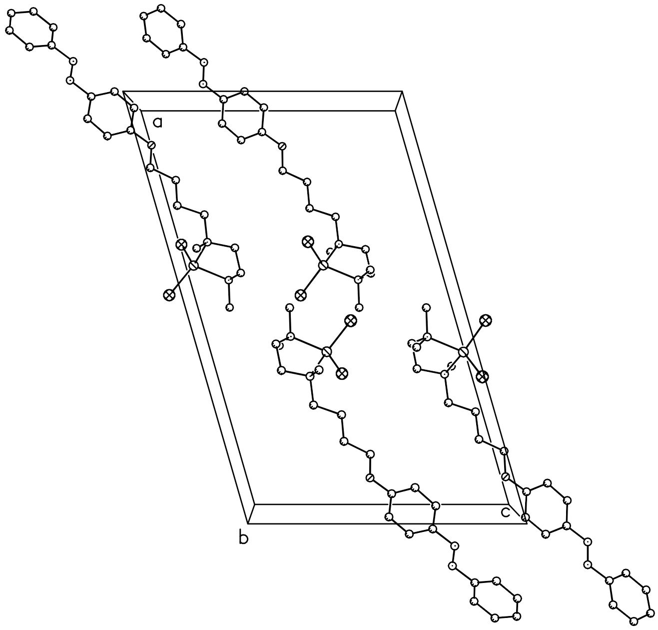

Fig. 4. The packing view along the *b*-axis of the complex **IIIa**.

force of the metal complex and the van der Waals force of the conjugated azobenzene group could be beneficial to the formation of the crystals.

3.4. Azobenzene isomerization reaction induced by UV light and thermal treatment

The azobenzene zinc chloride complexes were irradiated with UV light to explore their *trans-cis* isomerization phenomena. Figs. 5 and 6 show the UV absorbance changes of **IIIa** dilute solution (4.3×10^{-5} M, $\varepsilon = 2.3 \times 10^{6}$ M^{-1} m^{-1}) in toluene under the influence of UV irradiation and heat treatment respectively.

Before the azobenzene isomerization measurement, the sample solutions were kept in dark for several days at room temperature and at elevated temperature, about 70 °C, for several hours, to ensure that all of the azobenzene units were in *trans* form. This process could be monitored by observing the absorption peak increasing at 347 nm of *trans* form π–π^* transition until the absorbance reached a maximum value. One test showed that absorption peak at 347 nm of *trans* azobenzene increased about 20% by heat treatment at 70 °C for 2.0 h even after the solution sample already had been put in the dark for several days at room temperature. This phenomenon shows that heat treatment of sample in the dark can speed the isomerization to the more stable *trans* isomer and near hundred percent *trans* form azobenzene sample could be obtained as long as sufficient heat treatment provided.

Table 1
Crystal data and structure refinement for **IIIa**.

Empirical formula	$C_{21}H_{32}Cl_2N_4OZn$
Crystal system	Monoclinic
Formula weight	492.78
Wavelength	0.71073×10^{-1} nm
Space group	$P2_1/C$
Unit cell dimension	$a = 22.609$ Å, $\alpha = 90°$
	$b = 7.970$ Å, $\beta = 106.13°$
	$c = 14.054$ Å, $\gamma = 90°$
Volume, *Z*	2432.5 Å^3, 4
Density (calculated)	1.346×10^3 kg/m^3
Absorption coefficient	1.248×10^3 m^{-1}
F(000)	1032
Crystal size	$0.50 \times 0.40 \times 0.05$ m^{-3}
θ range for data collection	1.88–25.00°
Limiting indices	$-26 \le h \le 26$, $-9 \le k \le 1$, $-1 \le l \le 16$
Reflection collected	5600
Independent reflections	4294 ($R_{\text{int}} = 0.0386$)
Absorption correction	Semi-empirical from psi-scan
Refinement method	Full-matrix least squares on F^2
Goodness-of-fit on F^2	1.036
Final R indices [$I > 2\sigma$ (I)]	$R1 = 0.0554$, w$R2 = 0.1205$

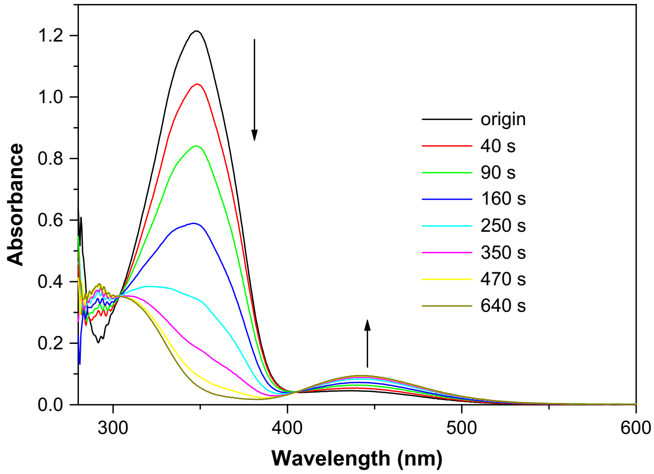

Fig. 5. UV absorbance changes of **IIIa** solution in toluene under 360 nm UV irradiation.

It can be seen from Figs. 5 and 6 that absorbance peak at 347 nm decreased and the peak at 440 nm increased as the solution samples were irradiated with UV light for different times due to *trans-cis* isomerization of azobenzene moiety. After saturated UV light irradiation, the *cis-trans* isomerization could be induced by thermal treatment in the dark. The sharp isosbestic points at 405 and 303 nm indicated that the azobenzene isomerization was the only process and is a reversible photo reaction. Preliminary tests showed that after more than ten cycles of UV light induced *trans-cis* and thermally induced *cis-trans* isomerization cycles, the peak values and positions were still maintained without noticeable change.

Another remarkable feature of these azobenzene containing metal complexes is their isomerization efficiency. The percentage of the *cis* isomer of the azobenzene molecules after saturated UV irradiation is a very important factor for both theoretical and application aspects. Assuming an initial all *trans* status, the *cis* isomer fraction after irradiation was determined from spectrophotometric absorbance by equation (1) [12].

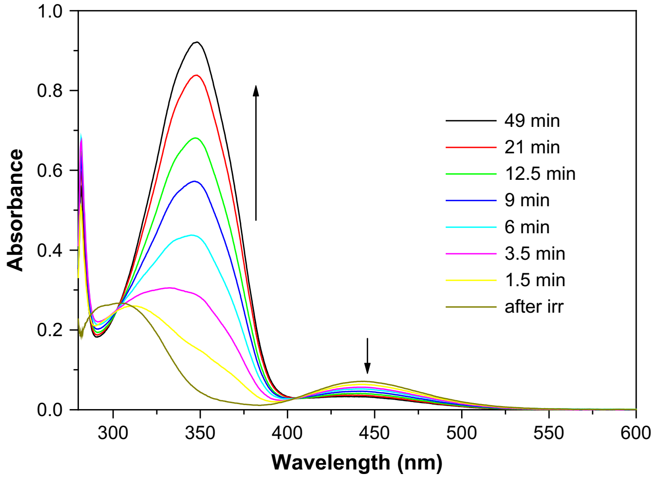

Fig. 6. UV absorbance changes of **IIIa** solution in toluene under 80 °C thermal treatment after saturated UV irradiation.

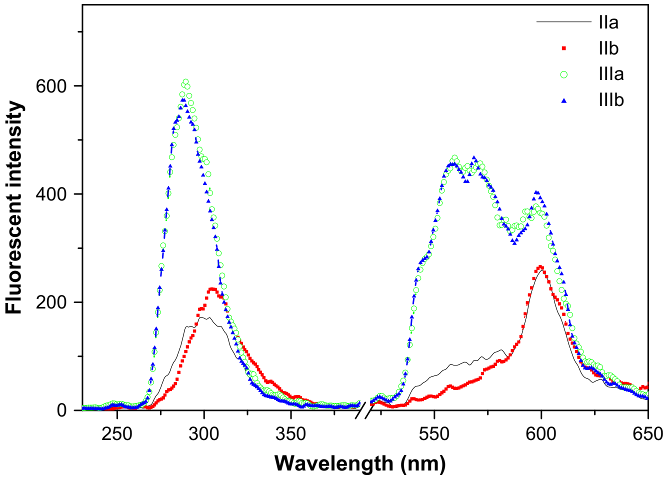

Fig. 7. Fluorescence emission spectra of **IIa**, **IIb**, **IIIa** and **IIIb** in acetonitrile solvent.

$$[Y]_{\mathrm{cis}} = \frac{1 - A/Ao}{1 - \varepsilon_{\mathrm{cis}}/\varepsilon_{\mathrm{trans}}} \qquad (1)$$

Where Ao is the initial absorbance of *trans* isomer at $\lambda_{\max}$ absorbance, A is the absorbance after saturated UV irradiation at the same wavelength, $\varepsilon_{\mathrm{cis}}$ and $\varepsilon_{\mathrm{trans}}$ are the molar absorption coefficients of the pure *cis* and *trans* isomers respectively, the ratio of $\varepsilon_{\mathrm{cis}}$ to $\varepsilon_{\mathrm{trans}}$, according to literature, is 0.055 for small azobenzene molecules [12].

The calculated results of $[Y]_{\mathrm{cis}}$ were between 99.2 and 99.4% of *cis* isomer after saturation with 360 nm UV light irradiation for the two azobenzene containing metal complexes in diluted toluene solution. The measurements and results could be repeated for many times without noticeable deviation. These values are remarkably higher than the published values of other azobenzene containing small molecules and polymers [12,13]. It is no doubt that such high isomerizing efficiency is advantageous to photo-switching related applications.

3.5. Fluorescence behavior of ligands and metal complexes

The fluorescence measurements were carried out on **IIa**, **IIb**, **IIIa** and **IIIb** samples in dilute acetonitrile solutions (7.0×10^{-6} M for **IIa** and **IIb** and 4.4×10^{-6} M for **IIIa** and **IIIb**). Fluorescence spectra are shown in Fig. 7, relative intensities of ligands and metal complexes are listed in Table 2. From Fig. 7 and Table 2, it can be seen that Chelation Enhanced Fluorescence (CHEF) from Zn^{2+} ion increases relative fluorescent intensity of compounds **IIa** and **IIb** more than four-fold. Similar CHEF effects were also reported from secondary amine ligands [14]. Noticeable features of the metal complexes **IIIa**, **b** are that two bands of emission centered at 290 nm and 560 nm respectively were found with a similar magnitude of fluorescent emission intensity as compared with that of ligands **IIa**, **b**. It is well known that the azobenzene moiety does not show any fluorescence because azobenzene is characterized by a shallow minima for singlet and triplet levels of both $\pi\pi^*$ and $n\pi^*$ electronic configuration, as a consequence, the non-irradiative processes, which include *trans-cis* inter-conversion, are very fast and compete efficiently with radiative process [15]. We tentatively propose that 290 nm band emission is due to Zn^{2+} ion induced CHEF effect similar to the reported results [16]. 560 nm band emission may be due to the azobenzene moiety, since it is bound to a relative heavy metal complex, its degree of distortion is reduced, which in turn reduces its non-radiative process and increases its radiative intensity around 560 nm.

Table 2
Relative fluorescent intensity of azobenzene ligands and metal complexes.[a]

Intensity[b]/$\lambda_{\max}$(nm)	Compounds			
	IIa	**IIb**	**IIIa**	**IIIb**
Band 1	1.00	1.05	4.30	4.23
$\lambda_{\max}$	303.0	304.5	298.5	288.0
Band 2	1.06	1.03	4.51	4.53
$\lambda_{\max}$	600.5	599.5	559.5	559.5

[a] Excitation wavelength: 200 nm.
[b] Fluorescent intensity values are based on integrated fluorescent intensities at the same concentration in acetonitrile, Band 1 is in the range of 260–360 nm; band 2 is in the range of 520–650 nm.

3.6. Holographic image formation

A tentative experiment to demonstrate holographic data storage inscription and readout based on compound **IIIa** in a polymeric matrix (PMMA) was successful. The experimental setup involves the routine dual laser beam interfering holographic grating formation setup [17]. Fig. 8 shows original and reconstructed holographic images of the word SINGAPORE and its emblem. The image was inscribed in a 150 µm thick PMMA film with 5.0 w% of **IIIa** evenly distributed throughout the matrix. The successful formation of holographic image by interfering laser beams is believed to be due to the unique multiphase formation/transition ability of **IIIa**. However **IIIb** was also tested under identical conditions but did not show any holographic inscription.

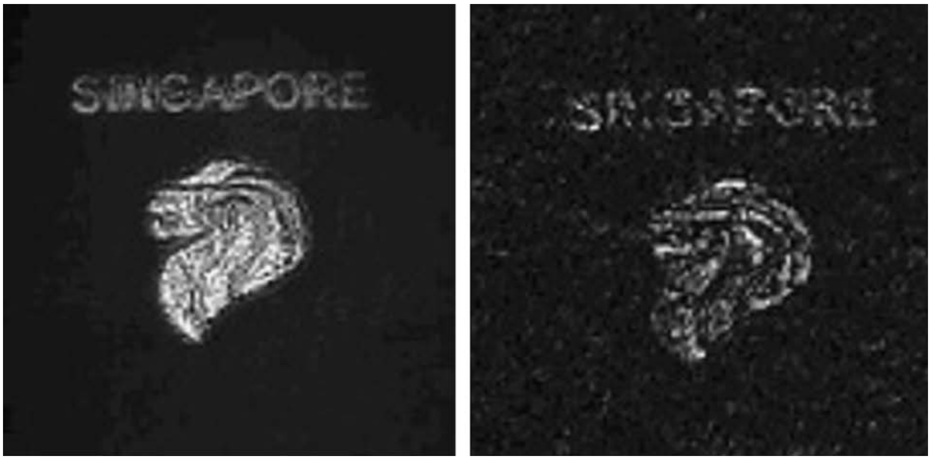

Fig. 8. Holographic image formation based on **IIIa** in PMMA matrices. Left is the original image to be constructed, right one is the reconstructed hologram of the recorded image.

4. Conclusions

In the summary, two novel azobenzene-containing metal complexes **IIIa**, **b** were successfully synthesized and characterized. It was revealed that these two compounds had quite noticeable different thermal and other properties arising from different spacer chain length connecting azobenzene chromophore and metal-complex. UV light and thermal treatment showed remarkable near hundred percent *trans-cis* and *cis-trans* isomerizing efficiency and this cycle was repeated 10 times without noticeable fatigue. Fluorescent measurements showed that a CHEF effect of more than 4 fold the fluorescence intensity increment of metal complexes was achieved. Two emission bands centered at 290 nm and 560 nm from metal complexes in solution were observed. A holographic image was successfully stored using **IIIa** in a polymeric matrix. These results show that an azobenzene moiety covalently linked to a metal complex by a hydrocarbon chain may afford various useful characteristics which may inspire practical applications.

Acknowledgements

We thank Dr Teng San Ong from Data Storage Institute of Singapore for the measurement of holographic image inscription and readout experiment.

References

[1] Natansohn A, Rochon P. Photoinduced motions in azo-containing polymers. Chemical Reviews 2002;102:4139–76.

[2] Muraoka T, Kinbara K, Kobayashi Y, Aida T. Light driven open-close motion of chiral molecular scissors. Journal of the American Chemical Society 2003;125:5612–3.

[3] Cheelham AG, Hutchings MG, Claridge TDW, Anderson HL. Enzymatic synthesis and photoswitchable enzymatic cleavage of a peptide-linked rotaxane. Angewandte Chemie International Edition 2006;45:1596–9.

[4] Nashihara H. Combination of redox- and photochemistry of azo-conjugated metal complexes. Coordination Chemistry Review 2005;249:1468–75.

[5] Ye ZH, De Boni L, Neves UM, Mendonça CR, Bu XR. Synthesis and two-photon absorption property of novel salen complexes incorporated with two pendant azo dyes. Tetrahedron Letters 2009;13:1371–3.

[6] Tang HS, Zhu N, Yan VWW. Tetranuclear macrocyclic gold(i) alkynyl phosphine complex containing azobenzene functionalities: a dual-input molecular logic with photoswitching behavior controllable via silver(I) coordination/decoordination. Organometallics 2007;26:22–5.

[7] Curie M, Babic D, Marinic Z, Pasa-Tolic L. Synthesis and characterisation of Pd(II) complexes with a derivative of aminoazobenzene: dynamic ^{1}H-NMR study of cyclopalladation reactions in DMF. Journal of Organometallic Chemistry 2003;687:85–99.

[8] Ghedini M, Pucci D, Crispini A, Barberio G. Oxidative addition to cyclometalated azobenzene platinum(ii) complexes: a route to octahedral liquid crystalline materials. Organometallics 1999;18:2116–24.

[9] Hu X, Zheng PJ, Zhao XY, Li L, Tam KC, Gan LH. Preparation, characterization and novel photoregulated rheological properties of azobenzene functionalized cellulose derivatives and their α–CD complexes. Polymer 2004;18: 6219–25.

[10] Zhao XY, Hu X, Yue CY, Xia XL, Gan LH. Synthesis, characterization and dual photochroic properties of azo-substituted polythiophene derivatives. Thin Solid Films 2002;417:95–100.

[11] Seshadri T, Haupt HJ. Thermotropic properties of monosubstituted ferrocene derivatives bearing bidentate *N*-benzoyl- *N*'-arylthiourea ligands—novel building blocks for heterometallic liquid crystal systems. Journal Of Materials Chemistry 1998;8(6):1345–50.

[12] Morishima Y, Tsuji M, Kamachi M. Photochromic isomerization of azobenzene moieties compartmentalized in hydrophobic microdomains in a microphase structure of amphiphilic polyelectrolytes. Macromolecules 1992;25:4406–10.

[13] Wang WY, Wang MZ. Effect of α-cyclodextrin on the photoisomerization of azobenzene functionalized hydroxypropyl methylcellulose in aqueous solution. Polymer Bulletin 2007;59:537–44.

[14] Inoue MB, Munoz IC, Inoue M, Fernando Q. X-ray structures and fluorescence spectra of binuclear Zn^{2+} and Cd^{2+} complexes of an amide-based naphthalenophane. Inorganica Chimica Acta 2000;300:206–11.

[15] Ghedini M, Pucci D, Crispini A, Aiello I, Barigelleli F. Dinuclear cyclopalladated azobenzene complexes: a comparative study on model compounds for organometallic liquid-crystalline materials. Applied Organometallic Chemistry 1999;13:565–81.

[16] Bernardo MA, Pina F, Garcia-Espana E, Latorre J, Luis SV, Llinares JM. Thermodynamic and steady-state fluorescence emission studies on metal complexes of receptors containing benzene subunits. Inorganic Chemistry 1998;37:3935–42.

[17] Manickasundaram S, Kannan P, Hassan QMA, Palanisamy PK. Azo dye based poly(alkyloxymethacrylate)s and their spacer effect on optical data storage. Journal of Materials Science: Materials in Electronics 2008;19: 1045–53.